Aquat. Sci. 65 (2003) 402–414
1015-1621/03/040402-13
DOI 10.1007/s00027-003-0675-4

Aquatic Sciences

Research Article

Role of the photo-Fenton reaction in the production of hydroxyl radicals and photobleaching of colored dissolved organic matter in a coastal river of the southeastern United States

Emily M. White, Pamela P. Vaughan and Richard G. Zepp*

Ecosystems Research Division, National Exposure Research Laboratory, USA
Environmental Protection Agency, 960 College Station Road, Athens, GA 30605-2700, USA

Received: 1 May 2003; revised manuscript accepted: 30 August 2003

Abstract. Photochemical reactions involving colored dissolved organic matter (CDOM) in natural waters are important determinants of nutrient cycling, trace gas production and control of light penetration into the water column. In this study the role of the hydroxyl radical (•OH) in CDOM photodegradation was explored as well as the contribution of photo-Fenton chemistry to •OH formation. Photochemically produced •OH was observed under aerobic and dioxygen-depleted conditions in highly colored, acidic natural water samples obtained from a freshwater reach of the Satilla River, a river in the southeastern United States. Net aerobic •OH formation along with the production of hydrogen peroxide and Fe(II) provided evidence of photo-Fenton produced •OH. A reduction in •OH production in the presence of iron chelators further suggests the importance of iron and the photo-Fenton reaction in this water. Apparent quantum yield values for the photochemical production of •OH were determined from 300–320 nm. In addition, the relationship between •OH photoproduction and effects of irradiation on the optical properties of CDOM was examined. Changes in the light absorption and fluorescence properties of water samples from the Satilla River and other natural waters were compared to •OH production rates. The ability of constituents of Satilla River water, principally the dissolved organic matter, to scavenge •OH was also considered. Results indicate that the photo-Fenton reaction accounts for more than 70% of total photochemical •OH production in Satilla River water. Given the significant levels of •OH produced in this water, it is possible that •OH influences CDOM photobleaching.

Key words. Fenton reaction; colored dissolved organic matter (CDOM); hydroxyl radical; photochemistry.

Introduction

Photochemical reactions involving colored dissolved organic matter (CDOM) in natural waters are important in terms of the cycling of carbon, nitrogen, and redox sensitive metals in the aquatic environment. In addition, photochemical degradation of CDOM can affect the penetration of light into the water column. Many reactive transients are produced through photochemical reactions in natural waters. The hydroxyl radical (•OH) is the most highly reactive of the many reactive oxygen species produced in these systems (Blough and Zepp, 1995). The production of •OH accompanies photoreactions of nitrate (Zafiriou and True, 1979; Zepp et al., 1987; Zellner et al., 1990), nitrite (Zafiriou and True, 1979; Zafiriou and Bonneau, 1987), iron and copper complexes (Zepp et al., 1992; Faust, 1994; Blough and Zepp, 1995; Voelker and Sulzberger, 1996; Goldstone et al., 2002; Zepp, 2002) and CDOM (Mopper and Zhou, 1990; Vaughan and Blough, 1998). Steady-state •OH concentrations can be calculated based on the major

* Corresponding author phone: (706) 355-8117;
fax: (706) 355-8104; e-mail: zepp.richard@epamail.epa.gov
Published on Web: December 18, 2003.

known •OH sources and sinks (Hoigné et al., 1989; Schwarzenbach et al., 1993). These estimates generally assume that nitrate is the major source while carbonate and DOM are the dominant •OH scavengers. While this may be valid for some waters, •OH concentrations can be under-predicted in systems where CDOM photolysis (reaction 1) and photo-Fenton processes (reactions 2 and 3) serve as significant sources of •OH. However, the importance of these production pathways has not been fully explored.

$$\text{CDOM} + h\nu \rightarrow \rightarrow \text{OH} \quad (1)$$

$$\text{Fe(III)} + h\nu \rightarrow \text{Fe(II)} \quad (2)$$

$$\text{Fe(II)} + \text{H}_2\text{O}_2 \rightarrow \text{Fe(III)} + {}^{\bullet}\text{OH} + \text{OH}^- \quad (3)$$

In this paper, Fe(II) is used to represent Fe^{2+} and its complexes and Fe(III) to denote Fe^{3+} and its complexes with DOM and other ligands.

Photochemical reactions can result in the reduction of Fe(III) through ligand-to-metal charge transfer (reaction 4), or through reaction of the complexes with superoxide ions (reaction 5) (Faust and Zepp, 1993; Faust, 1994; Voelker and Sedlak, 1995; Voelker and Sulzberger, 1996; Voelker et al., 1997; Gao and Zepp, 1998; Emmenegger et al., 2000). The production of superoxide/hydroperoxyl radicals ($HO_2/O_2^{\bullet-}$) proceeds through the photoreduction of dioxygen by CDOM (reaction 6), resulting in the formation of hydrogen peroxide (H_2O_2) via dismutation of $HO_2/O_2^{\bullet-}$ (reaction 7) (Cooper and Zika, 1983; Draper and Crosby, 1983; Cooper et al., 1988; Scully et al., 1996).

$$\text{Fe}^{3+} - (\text{DOM})_m + h\nu \rightarrow \text{Fe}^{2+} - \text{DOM}_{m-1} + \text{DOM}_{ox}^{+} \quad (4)$$

$$\text{Fe(III)} + \text{O}_2^{\bullet-} \rightarrow \text{Fe(II)} + \text{O}_2 \quad (5)$$

$$\text{CDOM} + h\nu + \text{O}_2 \rightarrow \text{DOM}_{ox} + \text{HO}_2/\text{O}_2^{\bullet-} \quad (6)$$

$$\text{HO}_2/\text{O}_2^{\bullet-} + \text{HO}_2/\text{O}_2^{\bullet-} \rightarrow \text{H}_2\text{O}_2 \quad (7)$$

The concurrent photochemical production of Fe(II) and H_2O_2 in natural waters suggests that the photo-Fenton reaction may be occurring in natural waters, particularly in highly colored, iron-rich, acidic waters.

Due to the complexity of DOM, iron-DOM complexes and the associated photochemistry, there has, of yet, been little direct evidence that this photo-Fenton mechanism is actually occurring in natural waters. Preliminary investigations of •OH production by direct photolysis of CDOM suggest that the photo-Fenton reaction may be of importance. Specifically, Vaughan and Blough (1998) observed a reduction in •OH production upon removal of H_2O_2 from Suwannee River fulvic acid (SRFA), suggesting that up to 50% of •OH production may be due to the photo-Fenton route (under aerobic conditions). Furthermore, the addition of 2 μM iron to SRFA enhanced •OH production, indicating that iron and iron-organic complexes may contribute to •OH production either directly or through photo-Fenton chemistry (White, 2000). In a more detailed study, Southworth and Voelker (2003) found that H_2O_2 production rates from the photolysis of SRFA dropped off upon addition of iron and that iron addition was accompanied by an increase in •OH production. These results provide evidence that the photo-Fenton reaction is responsible for a significant amount of •OH production in iron-rich solutions of humic substances, and that this photo-Fenton source is comparable to •OH production from direct photolysis of SRFA in this system (Southworth and Voelker, 2003).

In addition to the production of •OH and H_2O_2, absorption of solar radiation by CDOM results in the formation of other secondary photoproducts including: carbon dioxide and dissolved inorganic carbon species, carbon monoxide, and low-molecular weight organic compounds (Kieber et al., 1990; Valentine and Zepp, 1993; Miller and Zepp, 1995; Amon and Benner, 1996; Granéli et al., 1996; Miller and Moran, 1997; Moran and Zepp, 1997). Since CDOM is the primary light-absorbing species in aquatic systems, the optical properties of natural waters may be affected by its breakdown. Photochemical degradation of CDOM results in a decrease in absorption coefficients and fluorescence of natural waters (Del Vecchio and Blough, 2002; Zepp, 2002). It is not clear how, or even if, these processes are related since the mechanisms responsible for CDOM photobleaching are not well understood. However, in waters with high rates of •OH production, some of the bleaching may be due to reactions between DOM and •OH (Goldstone et al., 2002). •OH "scavenging" by DOM has been studied for a variety of natural waters and DOM isolates (Hoigné and Bader, 1978; Hoigné and Bader, 1979; Haag and Hoigné, 1985; Hoigné et al., 1989; Mopper and Zhou, 1990; Zepp et al., 1992; Haag and Yao, 1992; Brezonik and Fulkerson-Brekken, 1998; Westerhoff et al., 1999; Goldstone et al., 2002; Southworth and Voelker, 2003). In addition, it is assumed that •OH is the reactive species responsible for the formation of low molecular weight fragments and discoloration during the treatment of wastewater by ozonolysis or irradiation with H_2O_2 (Takahashi et al., 1995). •OH is also thought to be important in certain processes used for degradation of humic acids in the treatment of drinking water (Staehelin and Hoigné, 1985; Gjessing, 1991; Cooper et al., 1996; Wang et al., 2001). Therefore, similar inferences may be made about the photobleaching process in natural waters. While the connection between •OH and DOM bleaching has been investigated for Suwannee River fulvic and humic acids (Goldstone et al., 2002), this mechanism has not been fully explored in actual natural water samples.

In this study we determine the contribution of the photo-Fenton reaction to •OH production in a natural water sample. We measured photochemical production of •OH in water samples from a highly colored, acidic river (Satilla River, Georgia, USA) that contains high iron concentrations (typically > 10 μM) and in other water samples from the southeastern United States. Apparent quantum yield values (at 300–320 nm) were determined for •OH production under both aerobic and dioxygen-depleted conditions. Photochemical production of H_2O_2 and Fe(II) was also quantified to examine the potential role of these species in •OH production. The photo-Fenton pathway was effectively eliminated by removal of either dioxygen or reactive iron from the system. We have also investigated the role of •OH in the photobleaching of CDOM in natural water samples. Changes in absorption spectra, due to exposure to light, were measured to show that photochemically produced •OH could potentially affect the bleaching of a water sample.

Materials and methods

Chemicals

Boric acid (99.99%), sodium hydroxide (99.99%), sodium nitrite (99.99%), sodium dihydrogen phosphate (99.99%), dimethyl sulfoxide (DMSO, 99.9%), hydrogen peroxide, chloroform, and hydroxylamine hydrochloride were purchased from Aldrich. Fluorescamine, trizma base (tris(hydroxymethyl)amino-methane, 99.8%), and horseradish peroxidase (250 units/mg) were purchased from Sigma. Glacial acetic acid, HPLC grade methanol and acetonitrile, ferrous ammonium sulfate, sulfuric acid, ammonium acetate, and *p*-hydroxyphenylacetic acid (POHPAA) were purchased from Fisher. Potassium permanganate, ethylenediaminetetraacetate (EDTA), and ferric chloride were purchased from J. T. Baker. Hydroxylamine sulfate (99%), and 1,10-phenanthroline (99%) were purchased from Alfa chemicals. Ferrozine iron reagent was purchased from Kodak. Quinine sulfate dihydrate was purchased from Fluka. Sodium fluoride was purchased from Matheson Coleman and Bell. Desferrioxamine mesylate (Desferal, DFOM) was obtained from Novartis Pharmaceuticals Corporation. 3-amino-2,2,5,5,-tetramethyl-1-pyrrolidinyloxy free radical (3AP) was purchased from Fisher (Acros). Potassium hydrogen phthalate (KHP) was purchased from Nacalai Tesque (provided by Shimadzu). Valerophenone (99%) was purchased from TCI. A Barnstead Nanopure® Model D-7331 purification system provided water for all experiments. Satilla River water samples, collected in August 1999 (pH 5.9, 21.6 mg C/L, 5 mM Fe) and March 2001 (pH 6.9, 19.7 mg C/L, 13.6 mM Fe), were filtered with 0.6 mm heat-treated glass fiber filters, 0.2-mm polycarbonate membrane filters and stored in the dark at 4 °C. With some of the experiments, fluoride (0.100 M) or DFOM (0.100 mM) was added to Satilla River water and stirred for 18 hours prior to irradiation to allow the Fe(III) to exchange from DOM complexes to the fluoride or DFOM. Additional filtered water samples were available that had been collected from the Mississippi River Plume, mid-Hawk channel in the Florida Keys, and a stream in the McDonalds Branch basin of the New Jersey Pine Barrens. Nitrite solutions were made in 50 mM borate buffer (pH 8) and stored in the dark at 4 °C.

Apparatus

Absorption spectra were obtained with an Agilent Model 8453 diode array spectrophotometer. Total organic carbon measurements were made with a Shimadzu TOC 5050A analyzer, using a 100 mL injection volume. The high-performance liquid chromatography (HPLC) system, consisting of a Waters 515 HPLC pump, Shimadzu RF10AXL fluorescence detector (390 nm excitation, 490 nm emission, 15 nm bandpass), and a Beckman Ultrasphere ODS (5 μm, 4.6 mm × 15 cm) reversed phase HPLC column, was similar to that described previously (Vaughan and Blough, 1998). Chromatographic separations were performed isocratically, using a mobile phase of 70% methanol/30% sodium acetate (50 mM, pH 4.0), at room temperature with a flow rate of 1 mL/min and a 50 ml injection loop. A Shimadzu RF10AXL fluorescence detector (15 nm bandpass) with a 1 cm cuvette was used to measure natural water fluorescence and hydrogen peroxide. Fluorescence intensity (F) was measured (350 nm excitation, 450 nm emission) relative to a quinine sulfate standard (10 ppb in 0.1 N H_2SO_4) and is reported in normalized fluorescence units (NFU) where 1 ppb quinine sulfate is defined as 1 NFU (Hoge et al., 1993).

Analytical methods

Photochemically produced hydrogen peroxide was quantified using an adaptation of the POHPAA method (Kok et al., 1986; Miller and Kester, 1988). After irradiation, fluorometric reagent was added so that the samples contained 10 mM tris buffer, 100 μM POHPAA, and 400 mg/L horseradish peroxidase. The sample was adjusted to pH 11 with sodium hydroxide and H_2O_2 was quantified by fluorescence (315 nm excitation, 420 nm emission). To correct these measurements for the natural fluorescence of CDOM, calibration samples were prepared by adding H_2O_2 to unirradiated Satilla River water. Blanks consisted of unirradiated Satilla River water containing the fluorometric reagent and correspond to the amount of H_2O_2 present in the unirradiated water. Because Satilla River water is highly colored, it was necessary to correct the H_2O_2 results for the loss in background fluorescence over the irradiation period (compared to the unirradiated

standards). The production of photoreduced iron (Fe(II)) was measured using the ferrozine method (Stookey, 1970; Voelker and Sulzberger, 1996). The measurement was made immediately to prevent interference due to post-irradiation changes in Fe(II) concentrations. For determination of total Fe, a reducing agent (hydroxylamine hydrochloride) and ferrozine were added to the sample. The sample was then heated to boiling for 10 minutes to allow for complete reduction of Fe(III). After cooling, acetate buffer was added and absorbance was measured at 562 nm. Blanks consisted of Nanopure®-purified water containing ferrozine. Standards were prepared by dilution of ferrous ammonium sulfate. Determination of total iron in the August 99 sample was done using the phenanthroline method (Clesceri et al., 1998).

Photochemical •OH production was determined using the chemical probe system developed by Vaughan and Blough (1998). This method employs the reaction between •OH and dimethyl sulfoxide (DMSO, $k_{OH,\ DMSO} = 6.6 \times 10^9\ M^{-1}\ s^{-1}$ (Buxton et al., 1988)) to quantitatively produce a methyl radical (Eberhardt and Colina, 1988) which then reacts with an amino-nitroxide (3AP) (Kieber and Blough, 1990; Blough and Simpson, 1988; Kieber et al., 1992; Johnson et al., 1996) to produce a stable *O*-methylhydroxylamine. Following derivatization with fluorescamine, the *O*-methylhydroxylamine adduct is separated by reversed phase HPLC and quantified fluorometrically. For quantitative •OH measurements, a methyl radical adduct standard was prepared via the Fenton reaction and the fluorescence response calibrated by methods described previously (Vaughan and Blough, 1998; Li et al., 1997). •OH production rates measured under aerobic conditions were corrected for the presence of dioxygen ($[O_2] \approx 250\ \mu M$) which competes with 3AP for the methyl radical (Vaughan and Blough, 1998). Samples for •OH analysis contained 30 mM DMSO and 250 μM 3AP. All dioxygen-depleted samples were bubbled with nitrogen for 5 minutes prior to irradiation, and the samples remained sealed during the irradiation. After irradiation, an aliquot of sample (50 μL – 1 mL) was adjusted to pH 8.0 with borate buffer, followed by derivatization with 100 mL of 10 mM fluorescamine. It is important to note that this method quantifies cumulative •OH production over the course of the irradiation. This differs from measurement of Fe(II) and H_2O_2 concentrations, which result from the interaction of several competing reactions. In addition, it has been recently found that in addition to trapping free •OH, this technique also quantifies hydroxylating intermediates (Pochon et al., 2002). Therefore, in this paper, all reported values for •OH production include both free •OH and any species capable of transferring •OH. Experimental error was determined as the standard deviation of replicate measurements.

In order to compare results for different water samples, light screening factors (SF) were used to correct observed •OH formation rates (R_{obs}, $M\ s^{-1}$) for differences in inner filtering effects during irradiation according to the following equations (Zepp, 1982; Hu et al., 2002):

$$R_{corr} = \frac{R_{obs}}{SF} \tag{8}$$

$$SF = \frac{1 - 10^{-A_\lambda}}{2.303(A_\lambda)} \tag{9}$$

where R_{corr} is the corrected production rate ($M\ s^{-1}$) and A_λ is the absorbance at the irradiation wavelength. For a light source similar to solar irradiance, the maximum spectral overlap between the light source and the action spectrum for •OH photoproduction was close to 330 nm and so the SF for broadband irradiations in the solar simulator was approximately computed using average absorbance at 330 nm during the irradiation.

Irradiation conditions

Two irradiation systems were used during the course of these experiments (a monochromatic light source and a solar simulator broadband light source). For the monochromatic system, the output of a 1000 W Xe arc lamp was passed through a Spectral Energy Corp. monochromator, set to a bandpass of 6.6 nm, and directed onto a 1 cm quartz cell containing 3 ml of the sample solution. Light intensities were measured using a Optronics Model 730A spectroradiometer, calibrated using a valerophenone actinometer (40 μM) at 308 nm for 30 minutes to 1 hour (Zepp et al., 1998). Apparent quantum yields for •OH production at wavelength l ($F_{OH,\lambda}$) were calculated using the following equation:

$$\Phi_{OH,\lambda} = \frac{R_{OH,\lambda}}{I_\lambda\,(1-10^{-A\lambda})} \tag{10}$$

Where $R_{OH,\lambda}$ is the rate of •OH production (in molecules $cm^{-3}\ s^{-1}$), I_λ is the number of photons of light that enter the system per unit volume and unit time, and A_λ is the initial absorbance of the solutions at the irradiation wavelength. As a further check of proper lamp calibration, the quantum yield for photochemical •OH formation by nitrite was determined. Quantum yield values for •OH production by nitrite (1 mM in borate buffer, pH 8) were determined ($\Phi_{OH,308} = 0.087 \pm 0.004$ dioxygen-depleted; $= 0.074 \pm 0.004$ aerobic) and are in agreement with those determined previously ($\Phi_{308} = 0.071 \pm 0.009$ (Zellner et al., 1990) and $\Phi_{OH,308} = 0.062 \pm 0.005$ (dioxygen-depleted); 0.059 ± 0.005 (aerobic) (Vaughan and Blough, 1998)).

Broadband irradiations were carried out in an Atlas Suntest CPS solar simulator employing a Xe lamp. Samples were irradiated in a 1 cm quartz cuvette containing 3 ml of sample or in filled quartz tubes immersed in a

constant temperature water bath (25 °C). The spectral irradiance for this system was measured using an Optronics Model 750 spectroradiometer and has been reported elsewhere (Moran et al., 2000; Miller et al., 2002). The irradiance was close to that observed under mid-afternoon sunlight on a clear July day in Athens Georgia, USA (latitude 34°N).

Results and discussion

Evidence of photo-Fenton produced •OH

To determine if •OH was being produced through the photo-Fenton reaction in Satilla River water, cumulative concentrations of •OH were measured under aerobic and dioxygen-depleted conditions (Fig. 1). Results indicated that •OH photoproduction was more rapid in the aerobic system. This result is consistent with the reactions that were previously discussed. In the presence of dioxygen, $O_2^{\bullet-}$ is produced (reaction 6), presumably from one electron transfer from species present in natural waters such as, reduced metals (Moffett and Zika, 1983) or humic substances (Cooper and Zika, 1983). H_2O_2 is then formed from the disproportionation of $O_2^{\bullet-}$ (reaction 7). It is assumed that photochemical H_2O_2 production was minimal under dioxygen-depleted conditions. Because H_2O_2 is involved in the photo-Fenton reaction, the difference between aerobic and dioxygen-depleted •OH production should yield the contribution due to the photo-Fenton reaction alone, assuming that there are no differences in direct •OH production from CDOM under aerobic and dioxygen-depleted conditions. A comparison of total (aerobic) and non-photo-Fenton (dioxygen-depleted) produced •OH in Figure 1 indicates that the photo-Fenton reaction is responsible for at least 70% of total •OH production in Satilla River water. Because dioxygen likely was not completely removed from the water sample by the nitrogen saturation technique used here, it is possible that an even higher fraction of •OH photoproduction is attributable to photo-Fenton chemistry than is indicated by the data in this figure.

Additional experiments were conducted to obtain more information about the interrelationship between •OH production rates and changes in Fe(II) and H_2O_2 concentrations in the Satilla water samples. Photoproduction rates of •OH (R_{OH}, M s^{-1}) were computed for various time intervals using the aerobic data in Figure 1. The rates were with measured concentrations of Fe(II) and H_2O_2 in the irradiated water sample. The •OH production rates were dependent upon both Fe(II) and H_2O_2 as production initially increases at a faster rate while Fe(II) and H_2O_2 build up (Fig. 2). After about 25 minutes of total irradiation time, the H_2O_2 concentration and the •OH photoproduction rate have considerably dropped back from their maxima but still have not reached steady-state. After longer irradiation times, cumulative •OH production increased linearly with time, indicating that steady-state has been reached (Fig. 3).

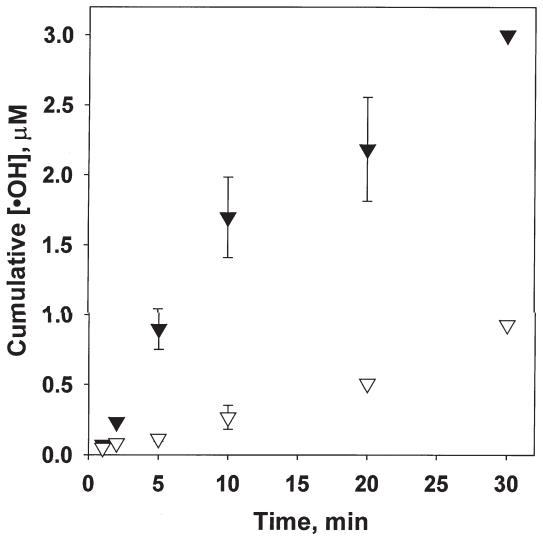

Figure 1. Cumulative photochemical production of •OH under aerobic (▼) and dioxygen-depleted (▽) conditions. For •OH measurement, samples contained 250 μM 3AP and 30 mM DMSO. All samples were irradiated in a 1 cm quartz cuvette in the solar simulator. A light screening factor was employed to correct for inner filter effects (eq. 9).

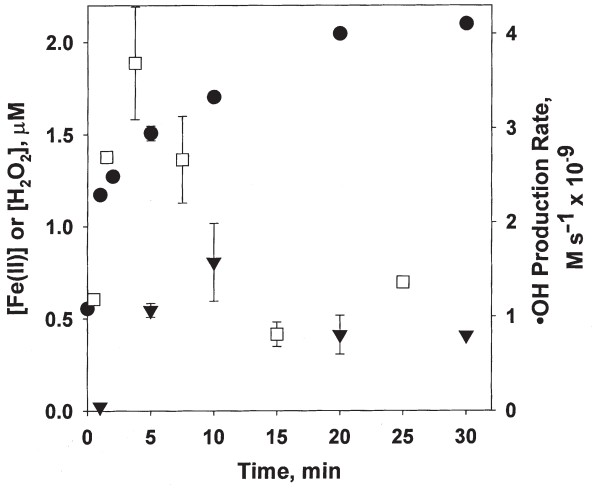

Figure 2. Concentrations of Fe(II) (●) and H_2O_2 (▼) compared to photoproduction rates of •OH (□) in irradiated Satilla River water. For determination of H_2O_2 and Fe(II), samples containing filtered Satilla River water (August 1999) were irradiated and then reagents were added for analysis. The •OH photoproduction rates were computed from the aerobic data shown in Figure 1. A light screening factor was employed to correct for inner filter effects (eq. 9). All samples were irradiated in a 1 cm quartz cuvette in the solar simulator. Sample conditions were identical to those in Figure 1.

To further investigate the importance of the photo-Fenton reaction in Satilla River water, the effects of adding Fe(III) complexing ligands were investigated. Fluoride and DFOM, two ligands that strongly complex

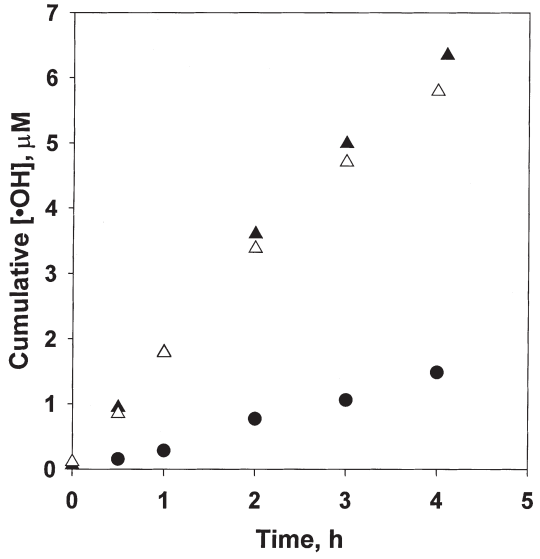

Figure 3. Photochemical production of •OH in Satilla River water (March 2001) (▲), Satilla River water containing 0.100 M fluoride (△) and Satilla River water containing 0.100 mM DFOM (●). For cumulative •OH measurement, samples containing 30 mM DMSO and 250 μM 3AP were irradiated in quartz tubes in the solar simulator under aerobic conditions. •OH production rates (corrected by SF) are 0.43 nM/s in Satilla River, 0.39 nM/s with fluoride, and 0.10 nM/s with DFOM.

Fe(III) (Hudson et al., 1992; Morel and Hering, 1993) were added with the intent of eliminating the photo-Fenton pathway by inhibiting Fe photoreduction through the formation of unreactive Fe(III) complexes (Gao and Zepp, 1998). Addition of DFOM to Satilla River water resulted in a significant (76%) reduction in photochemical •OH production while fluoride caused a decrease of less than 10% (Fig. 3). The degree of retardation by DFOM was closely consistent with the effects of dioxygen that were discussed earlier; both results were consistent with the hypothesis that a large fraction of the •OH photoproduction resulted from the photo-Fenton reaction. However, if the retarding effect were solely attributable to formation of unreactive Fe complexes, then the much greater effectiveness of DFOM compared to fluoride is not readily explicable. Other possible explanations for the retarding effect of these Fe(III) ligands on •OH photoproduction involve scavenging of •OH by the additives and/or inner filter effects caused by changes in light absorption by the added ligands and their Fe complexes.

(1) • OH scavenging-DFOM does react rapidly with •OH ($k_{OH, DFOM} = 1.3 \times 10^{10}$ $M^{-1}s^{-1}$ (Hoe et al., 1982)), and, in comparison, fluoride is stable to attack by •OH. Thus, the greater inhibition of detectable •OH by DFOM could be attributable in part to more efficient •OH scavenging by this ligand. However, given the fact that the DFOM concentration was much lower than that of DMSO used in the •OH detection system, it is unlikely that DFOM scavenging had a significant effect on our results. This was confirmed by conducting a control experiment in which nitrite photolysis was used as the source of •OH. With nitrite as the •OH source, 0.100 mM DFOM (or 0.100 M fluoride) had no detectable interference with the •OH detection system used here.

(2) Inner filter effects – The Fe(III)-DFOM complex absorbs at wavelengths >280 nm in the UV-visible region, whereas Fe(III)-fluoride complexes have no absorption in this spectral region. Thus, the greater inhibition of •OH photoproduction by DFOM potentially could be caused by more effective light screening by its complex with Fe(III). However, the maximum contribution of the Fe(III)-DFOM complex to absorption coefficients in the 280–350 nm region was < 0.02 cm^{-1}, or less than 5% of the absorption coefficients of the Satilla River water in this photochemically active UV region. Thus, the Fe(III)-DFOM complex had only minimal inner filter effects on photoproduction of OH radicals. Likewise, addition of 0.100 M fluoride only slightly reduced the absorption coefficients of the Satilla River water samples at wavelengths >280 nm, indicating little effect of added fluoride on inner filtering. The minimal effects of added fluoride on the Satilla absorption spectra indicate that Fe(III) absorption only made a small contribution to UV-visible light absorption in the samples.

Based on these considerations, we conclude that neither differential •OH scavenging or inner filter effects can account for the differences in effects of these Fe chelating ligands on •OH photoproduction in this system. Although both fluoride and DFOM inhibited •OH photoproduction, there were differences in the quantitative effects that will require additional experiments to explain.

In the absence of added Fe(III) ligands, H_2O_2 and Fe(II) reached steady-state concentrations of approximately 1.8 and 2.2 mM respectively, after about 30 minutes of irradiation (Figs. 4 and 5). Addition of fluoride effectively eliminated Fe(II) production while H_2O_2 accumulated to more than 5 mM in four hours (Figs. 4 and 5). Iron was also complexed in the presence of DFOM and the Fe(II) concentration remained below 1 μM during the irradiation period (Fig. 5). Oxidation of DFOM by horseradish peroxidase (Morehouse et al., 1987) prevented the determination of H_2O_2 in the sample containing DFOM by the method used in this study. These results indicate (in agreement with the dioxygen-depleted experiments) that the photo-Fenton reaction is responsible for a significant amount of the •OH produced in Satilla River water.

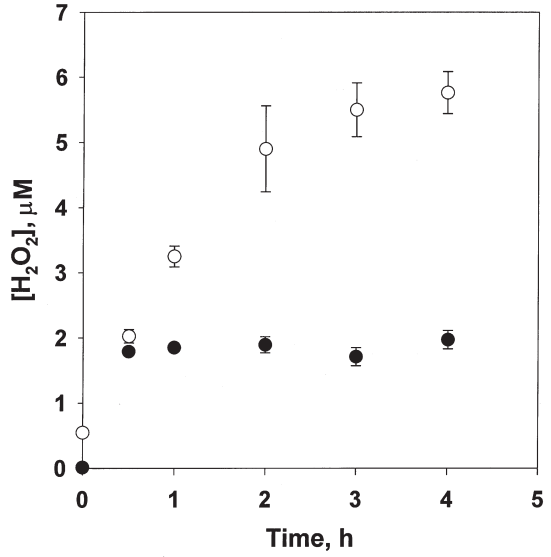

Figure 4. Buildup of H_2O_2 on irradiation of Satilla River water (March 2001) (●) and Satilla River water containing 0.100 M fluoride (○). Samples were irradiated in quartz tubes in the solar simulator under aerobic conditions.

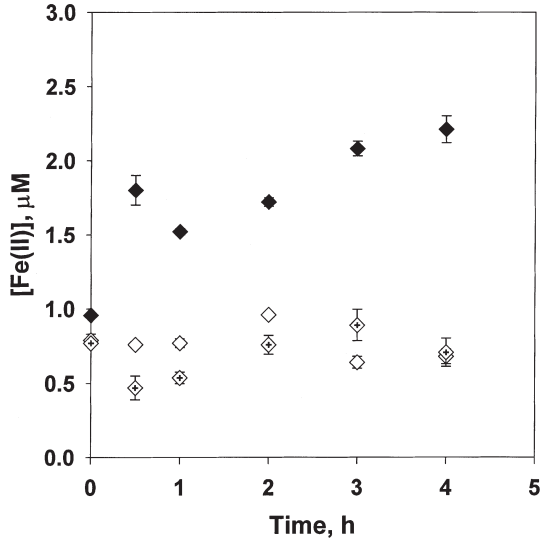

Figure 5. Photochemical production of Fe(II) in Satilla River water (March 2001) (◆), Satilla River water containing 0.100 M fluoride (◇) and Satilla River water containing 0.100 mM DFOM (◈). Samples were irradiated in quartz tubes in the solar simulator under aerobic conditions.

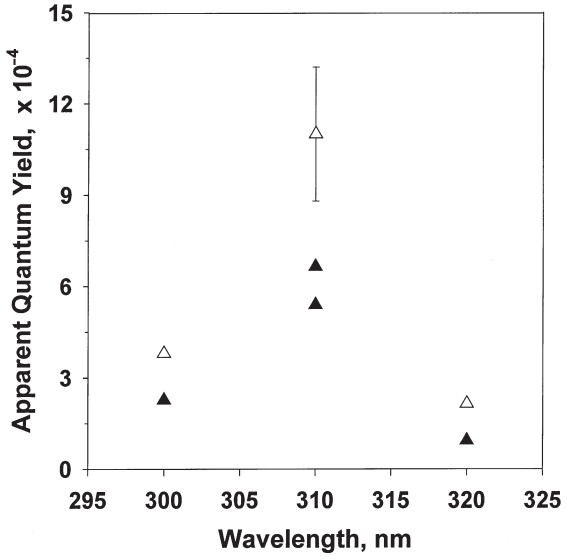

Figure 6. Apparent quantum yields for •OH production in Satilla River water under aerobic (△) and dioxygen-depleted (▲) conditions. Samples contained 5 mM phosphate buffer (pH = 5), 250 μM 3AP, 30 mM DMSO, and Satilla River water (August 1999) diluted to 7 mg C/L. Samples were irradiated for 1 hr by monochromatic radiation. The incident irradiance for these experiments was 0.22 mW/cm^2 at 300 nm, 0.30 mW/cm^2 at 310 nm, and 0.44 mW/cm^2 at 320 nm.

Wavelength dependence of the quantum yield

The wavelength dependence of the apparent quantum yield for photo-Fenton produced •OH was determined from equation 10. Using monochromatic light, Satilla River water samples were irradiated at 300, 310 and 320 nm under aerobic and dioxygen-depleted conditions for 1–2 hours (Fig. 6). In early monochromatic experiments, 5 mM phosphate (pH 5) was used to buffer the water samples. However, when unbuffered samples (pH 6) were irradiated, similar •OH production rates were observed. Fe(II)-phosphate complexes have been found to react with H_2O_2 to produce •OH (Blough, personal communication). Because phosphate complexation of Fe(III) can potentially influence Fenton chemistry (Moffett and Zafiriou, 1993; Gao and Zepp, 1998), unbuffered solutions were used for all remaining experiments.

The wavelength dependence of •OH photoproduction has been determined, to a limited extent, in coastal seawater samples and SRFA (Mopper and Zhou, 1990; Vaughan and Blough, 1998). The apparent quantum yields for Satilla River water in the 300 – 320 nm spectral region (Fig. 6) were about an order of magnitude higher than that observed for SRFA (Vaughan and Blough, 1998). Because it is a DOM isolate, SRFA is considered to be a known "organic" source of •OH. Yet, even for this organic source, some of the total •OH formation (< 50%) may be due to the photo-Fenton reaction (Vaughan and Blough, 1998). Southworth and Voelker (2003) found that the addition of DFOM to SRFA reduced •OH photoproduction. While, as suggested, some of this reduction observed with the •OH measurement system used by (Southworth and Voelker, (2003) may have been due to competitive scavenging of •OH (or other reactive transients) by DFOM, the exchange of iron associated with SRFA to DFOM may also have occurred, thus reducing •OH production by the photo-Fenton reaction. The close proximity of these iron complexes to the photoproduced H_2O_2 (within the DOM matrix) may enhance •OH production by the photo-Fenton pathway under conditions

(low iron and H_2O_2 concentrations) where it otherwise would not be important.

Because there are several mechanisms for •OH production in natural water samples, it is difficult to determine the individual contributions of each pathway to apparent quantum yield values. However, differences in the wavelength dependence and magnitude for various samples may indicate the involvement of different •OH production pathways. For example, the wavelength dependence of •OH production in Biscayne Bay water is likely representative of OH production from photolysis of CDOM as this is the major process involved in this water body (Mopper and Zhou, 1990). This differs from the wavelength dependence observed for SRFA (Vaughan and Blough, 1998) and Satilla River water (Fig. 6), especially for wavelengths less than 310 nm where Mopper and Zhou saw a dramatic increase in quantum yield with decreasing wavelength. This perhaps indicates a different mechanism for •OH production in SRFA and Satilla River water as compared to Biscayne Bay water (i.e., the photo-Fenton reaction). Aside from being more efficient at the wavelengths studied, the quantum yield spectrum for Satilla River water is similar to that observed for SRFA. Both show a maximum at 310 nm for •OH production under aerobic conditions as well as a maximum for the difference between aerobic and dioxygen-depleted production. This suggests that the photo-Fenton reaction is most efficient at 310 nm. Apparent quantum yield values were determined at 310 nm over different irradiation times (Table 1). Despite an initial enhancement with irradiation time, there appeared to be no further increase in the apparent quantum yield for •OH production after one hour. Comparison of the difference in apparent quantum yields for aerobic and dioxygen-depleted •OH production shows that the photo-Fenton pathway is more efficient in Satilla River water (4.35×10^{-4}) than in SRFA (5.5×10^{-5}, Vaughan and Blough, 1998).

Optical properties of CDOM

The electronic absorption spectra of most CDOM show exponential decreases in the ultraviolet and visible wavelength ranges (Blough and Green, 1995). In order to characterize the absorption properties of water samples, these spectra are fit to the following exponential form:

$$a_\lambda = a_{\lambda_0}\, e^{-S(\lambda-\lambda_0)} \tag{11}$$

Where a_λ is the absorption coefficient (m^{-1}) at wavelength λ, a_{λ_0} is the absorption coefficient at reference wavelength λ_0 (440 nm), and S is the spectral slope coefficient (from 290–700 nm). S characterizes how rapidly the absorption decreases with increasing wavelength. a_λ is determined from the sample absorbance (A_λ) and pathlength (r) (typically in meters) according to the following equation.

$$a_\lambda = \frac{2.303\, A_\lambda}{r} \tag{12}$$

The specific absorption coefficient, $a^*(\lambda)$ [L (mg org. C)$^{-1}$ m^{-1}], is the absorption coefficient normalized to the organic carbon concentration of the sample.

To characterize the bleaching of Satilla River water, samples were irradiated in the solar simulator for 30 hours. Absorption coefficients and fluorescence were measured to determine how the optical properties of the water change over time. The results were generally similar to those that have been previously reported for Satilla irradiations (Moran et al., 2000). Photobleaching was observed as a decrease in absorption coefficients over the entire spectrum. A small decrease in S (less than 5% in 30 hours) was observed with increasing irradiation time, in agreement with previous findings (Gao and Zepp, 1998; Moran et al., 2000). This decrease in S is slightly more rapid in the visible region (at $\lambda > 412$ nm where the slope is smaller). Fluorescence intensity decreased by approximately 50% after 30 hours of irradiation. This fluorescence loss was roughly first-order, with a bleaching rate of 1.8×10^{-5} s^{-1} for the first six hours of irradiation. In order to begin to look at the possible involvement of •OH in the photobleaching of natural waters, the decrease in absorption coefficients and fluorescence was measured in several natural water samples with varying •OH production rates.

•OH production rates (R_{OH}) were determined for Satilla River water as well as bleached Satilla River water and water samples from the New Jersey Pine Barrens, Mississippi River Plume, and the Florida Keys. These production rates were found to be within the range of previously reported values (Table 2). •OH production in the Satilla River water (4×10^{-10} M s^{-1}) agrees with that found for other similar waters from the southeastern US, the Ogeechee River (White, 2000) and the Everglades (Mopper and Zhou, 1990). The •OH production rate in the New Jersey Pine Barrens sample was very high (10^{-9} M s^{-1}), approaching that observed in waters contaminated with acid mine drainage (Allen et al., 1996). •OH pro-

Table 1. Apparent quantum yields for •OH production in Satilla River water (August 1999) under aerobic and dioxygen-depleted conditions at 310 nm.

Irradiation time (min)	Quantum yield (aerobic)	Quantum yield (dioxygen-depleted)
30	5.1×10^{-4}	
60	$1.0 \pm 0.2 \times 10^{-3}$	6.5×10^{-4}
120	1.2×10^{-3}	6.8×10^{-4}

Table 2. Reported rates of •OH production (R_{OH}) for various natural water samples.

Study	Water sample	R_{OH} ($M\ s^{-1}$)
This study	Satilla River	4.5×10^{-10}
	Satilla River (bleached)	2.0×10^{-10}
	Pine Barrens	1.7×10^{-9}
	Mississippi River Plume	6.2×10^{-11}
	Florida Keys	4.3×10^{-12}
Qian et al., 2001	Weddell Sea	1.04×10^{-12}
	Crystal Sound	1.03×10^{-12}
	Paradise Harbor	1.60×10^{-12}
White, 2000	Wetland on Lake Erie	$2 - 6 \times 10^{-10}$
	SRFA	0.6×10^{-10}
	Artificial agricultural wetland	2.3×10^{-10}
	Ogeechee River	2.4×10^{-10}
Allen et al., 1996	Surface waters contaminated with acid mine drainage	4.4×10^{-9} $- 7.4 \times 10^{-8}$
Mabury, 1993	Rice Field water	6.4×10^{-11}
	Clear Lake	4.6×10^{-11}
	Lake Tahoe	2.2×10^{-11}
Mopper and Zhou, 1990	Sargasso Sea	2.8×10^{-12}
	Gulf Stream	3.1×10^{-12}
	Biscayne Bay	2.9×10^{-11}
	Vineyard Sound	2.65×10^{-11}
	Everglades	4.20×10^{-10}
Zepp et al., 1987	Greifensee	2.5×10^{-11}
	Nitrate-rich shallow water body	1.8×10^{-13}
Haag and Hoigné, 1985	Greifensee	1×10^{-11}

duction in Mississippi River Plume water was on the same order of magnitude (10^{-11} M s^{-1}) as waters from Biscayne Bay and Vineyard Sound (Mopper and Zhou, 1990) as well as various lakes (Haag and Hoigné, 1985; Zepp et al., 1987; Mabury, 1993). The Florida Keys sample had a lower rate of •OH production (10^{-12} M s^{-1}), similar to samples from Antarctic waters (Qian et al., 2001) as well as the Gulf Stream and the Sargasso Sea (Mopper and Zhou, 1990).

Experimentally determined rates of •OH production were normalized to the absorption coefficient at 350 nm (a_{350}) in order to directly compare different water samples (Hu et al., 2002). The results of these bleaching experiments are shown in Table 3 and the changes in absorption spectra due to irradiation are shown in Figure 7. As with the Satilla River sample, S decreased upon irradiation of the Pine Barrens water. These two waters have similar absorption spectra (Fig. 7). However absorption bleaching was faster in the Pine Barrens sample. Both of these samples are highly colored and high in iron. The photo-Fenton reaction is likely to be very important in the Pine Barrens sample (pH 4, 25 mg C/L, 14 mM Fe) especially due to its low pH. Fluorescence bleaching was much less dramatic in the Pine Barrens sample and was found to de-

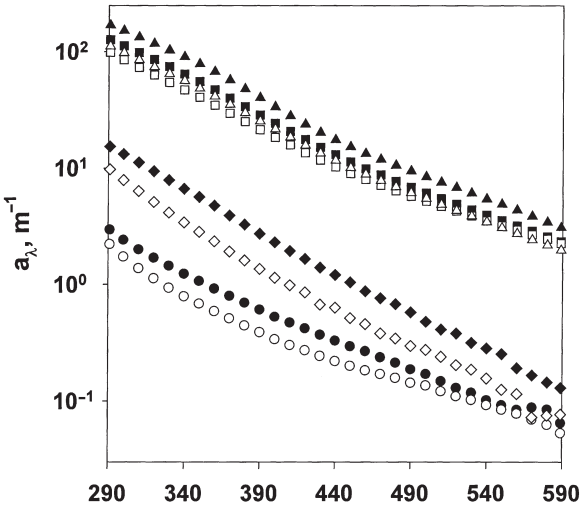

Figure 7. Absorption spectra of Pine Barrens (▲), Satilla River (■), Florida Keys (●), and Mississippi River Plume (◆) water, before and after (open symbols) 18 hours of broadband irradiation.

crease linearly with irradiation time. Despite this lower loss rate of fluorescence, the Pine Barrens sample had a very large rate of •OH production. The other two samples, from the Mississippi River Plume and the Florida Keys, showed a very small increase in S after irradiation. However the decrease in absorption coefficients for these samples was comparable to that seen for the water samples from the Satilla River and Pine Barrens. Bleaching of fluorescence in the Mississippi River Plume sample was more efficient than in Satilla River water. Except for the Mississippi River Plume sample, there is a general trend that when bleached, samples with larger •OH production rates experience larger decreases in S (Table 3). S values for samples with small rates of •OH production, such as the Florida Keys sample, were observed to increase after irradiation. The Mississippi River Plume sample probably contains a major non-DOM source of •OH (most likely, nitrate or nitrite). Therefore, normalization of the •OH production rate to a_{350} likely overestimates the CDOM contribution to •OH photoproduction. Based on these results, it appears that •OH may be involved in the bleaching process and may influence how S changes due to irradiation. To further explore the importance of this relationship, it will be useful to examine •OH photoproduction and changes in S in additional samples. Different natural water samples do not have the same response to photobleaching. In the samples studied here, we observed small changes in S. However, other studies have observed different changes in S as a result of irradiation. For example, Del Vecchio and Blough (2002) saw larger increases in S for SRFA and Delaware Bay water. The observed differences in the change in S of various samples suggest that the photobleaching of all natural water samples may not be the same. However, given the complexity

Table 3. Optical properties and rates of photochemical bleaching and •OH production in natural water samples. Samples were irradiated for 18 hours (the Florida Keys sample was irradiated for 20 hours) in the solar simulator. Bleaching rates were determined for decreases in absorption coefficients (k_a) and fluorescence (k_f) at 350 nm over the first six hours of irradiation. •OH production rates (R_{OH}*), based on measurements taken over a four hour irradiation period, have been corrected by the screening factor and normalized to a_{350}. †Bleaching of fluorescence in the Pine Barrens sample was zero order with a bleaching rate of 2.9×10^{-4} NFU s^{-1}.

Sample	S	ΔS	a (m^{-1})	k_a (s^{-1})	Δa (%)	F (NFU)	k_f (s^{-1})	ΔF (%)	R_{OH}* ($\times 10^{-11}$ M s^{-1} m)
Satilla	0.0155	−0.00036	55.2	6.8×10^{-6}	−27	124.8	2.6×10^{-6}	−53	0.81 ± 0.06
Satilla (bleached)	0.0151		40.5			70.1			0.50 ± 0.04
Pine Barrens	0.0156	−0.00053	78.5	1.0×10^{-5}	−38	128.0	†	−25	2.2 ± 0.2
Mississippi River Plume	0.0171	0.00023	5.7	1.1×10^{-5}	−50	31.3	4.9×10^{-6}	−71	1.09 ± 0.08
Florida Keys	0.0140	0.00030	1.07		−36	3.18			0.4

of CDOM and the resulting photochemistry when CDOM is irradiated with polychromatic light, it is difficult to isolate the mechanism responsible for photobleaching.

The potential interaction of •OH and photobleaching was investigated by measuring the rate constant for natural scavenging (k_{ns}) of •OH by Satilla River water. By measuring •OH production in samples containing a range of DMSO concentrations, the amount of DMSO needed to out compete natural •OH scavengers can be found. The kinetics are described by eq. (13):

$$R_p = \frac{R_{OH} k_p [P]}{(k_p [P] + k_{ns} [ns])} \quad (13)$$

Where R_p (M s^{-1}) is the rate of the reaction of the chemical probe (e.g., DMSO) with •OH, R_{OH} (M s^{-1}) is the hydroxyl radical production rate, k_p (M^{-1} s^{-1}) is the •OH scavenging rate constant of the probe (P), [P] is the probe concentration (M) added to the sample, k_{ns} is the •OH scavenging rate constant [L (mg org. C)$^{-1}$ s^{-1}] of natural organic scavengers in the water sample, and [ns] is the concentration of natural organic scavengers (mg org. C/L^{-1}). Assuming that the amount of scavengers and the scavenging rate remain constant, R_p will approach R_{OH} when $k_p[P] \gg k_{ns}[ns]$. The probe concentration required to satisfy this condition can be determined by measuring •OH production over a range of probe concentrations. Taking the reciprocal of equation 13 produces a linear form of this relation:

$$\frac{1}{R_p} = \frac{1}{R_{OH}} + \frac{k'_{ns}}{R_{OH} \times k_p} \times \frac{1}{[P]} \quad (14)$$

where $k'_{ns} = k_{ns}[ns]$.

Using this method, a value of 1.09 (± 0.07) × 10^{10} $M^{-1}s^{-1}$ was determined for the scavenging rate constant ($k_{OH, NO2}$) of nitrite. This value is in good agreement with the reported rate constant of 1.1×10^{10} $M^{-1}s^{-1}$ (Buxton et al., 1988). The natural scavenging rate constant (k_{ns}), or rate constant for the reaction of •OH with constituents of the water sample was found to be 2.3 (± 0.3) × 10^6 s^{-1} for the Satilla River water (March 2001). Assuming that the rate constant quantitatively involves reaction of •OH with the dissolved organic matter, the second order rate constant for •OH with Satilla DOM is 1.1 (± 0.15) × 10^5 L (mg org. C)$^{-1}$ s^{-1}. This value is within a factor of 2 of the range of second order rate constants that have been reported by others for reaction of •OH with DOM (Southworth and Voelker, 2003). The rate of photochemical •OH production for this Satilla River water sample was 0.31 (± 0.02) nM s^{-1}. After bleaching (by broadband irradiation for 18 hours), both the rate of •OH production and the natural scavenging rate constant decreased to 0.15 (± 0.01) nM s^{-1} and 1.6 (± 0.2) × 10^6 s^{-1} respectively. When corrected by the screening factor and normalized to a_{350}, this corresponds to a 38% decrease in •OH production and a 14% decrease in the •OH scavenging rate constant.

Conclusions

The results presented here show that the high rate of photochemical •OH formation in Satilla River water (0.4 nM s^{-1}) is largely due to the involvement of the photo-Fenton reaction.

Our findings suggest that this mechanism for •OH production also is important in other iron-rich natural waters that are mildly acidic. For example, waters which receive acid mine drainage will likely have high steady-state •OH concentrations due to photo-Fenton production (Allen et al., 1996; McKnight et al., 1988). In waters with high rates of •OH photoproduction it seems likely that •OH may play a significant role in the photoreactions of CDOM and aquatic pollutants.

Acknowledgments

We thank H. Xie for supplying Satilla River water, Y-P. Chin for providing the New Jersey Pine Barrens sample and R. Chen for providing the Mississippi River sample. An EPA National Network for Environmental Management Studies (NNEMS) Fellowship supported E.M.W. A NRC Postdoctoral Fellowship supported P.P.V. The research was supported in part by a grant from the Office of Naval Research to R. Zepp (N00014-98-F-0202). This paper has been reviewed in accordance with the U.S. Environmental Protection Agency's peer and administrative review policies and approved for publication. Mention of trade names or commercial products does not constitute an endorsement or recommendation for use by the U.S. EPA.

References

Allen, J. M., S. Lucas and S. K. Allen, 1996. Formation of hydroxyl radical in illuminated surface waters contaminated with acid mine drainage. Environmental Toxicology and Chemistry **15:** 107–113.

Amon, R. M. W. and R. Benner, 1996. Photochemical and microbial consumption of dissolved organic carbon and dissolved oxygen in the Amazon River system. Geochimica et Cosmochimica Acta **60:** 1783–1792.

Blough, N. V. and D. J. Simpson, 1988. Chemically mediated fluorescence yield switching in nitroxide-fluorophore adducts: optical sensors of radical/redox reactions. Journal of the American Chemical Society **110:** 1915–1917.

Blough, N. V. and S. A. Green, 1995. Spectroscopic characterization and remote sensing of nonliving organic matter. In: R. G. Zepp and C. Sonntag (eds.), The Role of Nonliving Organic Matter in the Earth's Carbon Cycle, John Wiley and Sons, New York, pp. 23–45.

Blough, N. V. and R. G. Zepp, 1995. Reactive oxygen species in natural waters. In: C. S. Foote, J. S. Valentine, A. Greenberg and J. F. Liebman (eds.), Active Oxygen in Chemistry, Blackie Academic and Professional, New York, pp. 280–333.

Brezonik, P. L. and J. Fulkerson-Brekken, 1998. Nitrate-induced photolysis in natural waters: controls on concentrations of hydroxyl radical photo-intermediates by natural scavenging agents. Environmental Science and Technology **32:** 3004–3010.

Buxton, G. V., C. L. Greenstock, W. P. Helman and A. B. Ross, 1988. Critical review of rate constants for reactions of hydrated electrons, hydrogen atoms and hydroxyl radicals in aqueous solution. Journal of Physical Chemistry Reference Data **17:** 513–886.

Clesceri, L., A. Greenberg, A. Eaton and M. A. Franson, 1998. Phenanthroline Method. In: Standard Methods for the Examination of Water and Wastewater, APHA, AWWA and WEF, Washington, DC, pp. 76–78.

Cooper, W. J. and R. G. Zika, 1983. Photochemical formation of hydrogen peroxide in surface and ground waters exposed to sunlight. Science **220:** 711–712.

Cooper, W. J., R. G. Zika, R. G. Petasne and J. M. C. Plane, 1988. Photochemical formation of hydrogen peroxide in natural waters exposed to sunlight. Environmental Science and Technology **22:** 1156–1160.

Cooper, W. J., K. L. Sawal, Y. S. Hoogland, R. Slifker, M. G. Nickelsen, C. N. Kurucz and T. D. Waite, 1996. Disinfection by-product precursor removal from natural waters using gamma radiation to simulate an innovative water treatment process. In: R. A. Minear and G. L. Amy (eds.), Disinfection By-Products in Water Treatment, CRC Press, Inc., Boca Raton, FL, pp. 151–162.

Del Vecchio, R. and N. V. Blough, 2002. Photobleaching of chromophoric dissolved organic matter in natural waters: kinetics and modeling. Marine Chemistry **78:** 231–253.

Draper, W. M. and D. G. Crosby, 1983. The photochemical generation of hydrogen peroxide in natural waters. Archives of Environmental Contaminant Toxicology **12:** 121–126.

Eberhardt, M. K. and R. Colina, 1988. The reaction of OH radicals with dimethyl sulfoxide. A comparative study of Fenton's reagent and the radiolysis of aqueous dimethyl sulfoxide solutions. Journal of Organic Chemistry **53:** 1071–1074.

Emmenegger, L., R. Schwarzenbach, L. Sigg and B. Sulzberger, 2000. Light-induced redox cycling of iron in circumneutral lakes. Limnology and Oceanography **46:** 49–61.

Faust, B. C. and R. G. Zepp, 1993. Photochemistry of aqueous iron(III)-polycarboxylate complexes: roles in the chemistry of atmospheric and surface waters. Environmental Science and Technology **27:** 2517–2522.

Faust, B. C., 1994. A review of the photochemical redox reactions of iron(III) species in atmospheric, oceanic, and surface waters: influences on geochemical cycles and oxidant formation. In: G. R. Helz, R. G. Zepp and D. G. Crosby (eds.), Aquatic and Surface Photochemistry, Lewis Publishers, pp. 3–38.

Gao, H. and R. G. Zepp, 1998. Factors influencing photoreactions of dissolved organic matter in a coastal river of the southeastern United States. Environmental Science and Technology **32:** 2940–2946.

Gjessing, E. T., 1991. Algicidal and chemical effect of UV radiation of water containing humic substances. Water Research **25:** 491–494.

Goldstone, J. V., M. J. Pullin, S. Bertilsson and B. M. Voelker, 2002. Reactions of hydroxyl radical with humic substances: bleaching, mineralization, and production of bioavailable carbon substrates. Environmental Science and Technology **36:** 364–372.

Granéli, W., M. Lindell and L. Tranvik, 1996. Photo-oxidative production of dissolved inorganic carbon in lakes of different humic content. Limnology and Oceanography **41:** 698–706.

Haag, W. R. and J. Hoigné, 1985. Photo-sensitized oxidation in natural water via hydroxyl radicals. Chemosphere **14:** 1659–1671.

Haag, W. R. and C. C. D. Yao, 1992. Rate constants for reaction of hydroxyl radicals with several drinking water constituents. Environmental Science and Technology **26:** 1005–1013.

Hoe, S., D. A. Rowley and B. Halliwell, 1982. Reactions of ferrioxamine and desferrioxamine with the hydroxyl radical. Chemical and Biological Interactions **41:** 75–81.

Hoge, F. E., A. Vodacek and N. V. Blough, 1993. Inherent optical properties of the ocean: retrieval of the absorption coefficient of chromophoric dissolved organic matter from fluorescence measurements. Limnology and Oceanography **38:** 1394–1402.

Hoigné, J. and H. Bader, 1978. Ozone and hydroxyl radical-initiated oxidations of organic and organometallic trace impurities in water. In: F. E. Brinkman and J. M. Bellama (eds.), Organometals and Organometalloids. Ocurrence and Fate in the Environment, pp. 292–313.

Hoigné, J. and H. Bader, 1979. Ozonation of water: oxidation-competition values of different types of waters used in Switzerland. Ozone Science and Engineering **1:** 357–372.

Hoigné, J., B. C. Faust, W. R. Haag, F. E. Scully, Jr. and R. G. Zepp, 1989. Aquatic humic substances as sources and sinks of photochemically produced transient reactants. In: I. H. Suffett and P. MacCarthy (eds.), Aquatic Humic Substances: Influence on Fate and Treatment of Pollutants, pp. 363–381.

Hu, C., F. E. Muller-Karger and R. G. Zepp, 2002. Absorbance, absorption coefficient, and the apparent quantum yield: A comment on common ambiguity in the use of these optical concepts. Limnology and Oceanography **47:** 1261–1267.

Hudson, R. J. M., D. T. Covault and F. M. M. Morel, 1992. Investigations of iron coordination and redox reactions in seawater using iron-59 radiometry and ion-pair solvent extraction of amphiphilic iron complexes. Marine Chemistry **38:** 209–235.

Johnson, C. G., S. Caron and N. V. Blough, 1996. Combined liquid chromatography/mass spectrometry of the radical adducts of a fluorescamine-derivatized nitroxide. Analytical Chemistry **68:** 867–872.

Kieber, D. J. and N. V. Blough, 1990. Determination of carbon-centered radicals in aqueous solution by liquid chromatography with fluorescence detection. Analytical Chemistry **62:** 2275–2283.

Kieber, D. J., C. G. Johnson and N. V. Blough, 1992. Mass spectrometric identification of the radical adducts of a fluorescamine-derivatized nitroxide. Free Radical Research Communications **16:** 35–39.

Kieber, D. J., X. Zhou and K. Mopper, 1990. Formation of carbonyl compounds from UV-induced photodegradation of humic substances in natural waters: fate of riverine carbon in the sea. Limnology and Oceanography **35:** 1503–1515.

Kok, G. L., K. Thompson, A. L. Lazrus and S. E. McLaren, 1986. Derivatization technique for the determination of peroxides in precipitation. Analytical Chemistry **58:** 1192–1194.

Li, B., P. L. Gutierrez and N. V. Blough, 1997. Trace determination of hydroxyl radical in biological systems. Analytical Chemistry **69:** 4295–4302.

Mabury, S. A., 1993. Hydroxyl radical in natural waters. Ph.D dissertation, University of California, Davis, California.

McKnight, D. M., B. A. Kimball and K. E. Bencala, 1988. Iron photoreduction and oxidation in an acidic mountain stream. Science **240:** 637–640.

Miller, W. L. and D. R. Kester, 1988. Hydrogen peroxide measurement in seawater by (p-hydroxyphenyl)acetic acid dimerization. Analytical Chemistry **60:** 2711–2715.

Miller, W. L. and R. G. Zepp, 1995. Photochemical production of dissolved inorganic carbon from terrestrial organic matter: significance to the oceanic organic carbon cycle. Geophysical Research Letters **22:** 417–420.

Miller, W. L. and M. A. Moran, 1997. Interaction of photochemical and microbial processes in the degradation of refractory dissolved organic matter from a coastal marine environment. Limnology and Oceanography **42:** 1317–1324.

Miller, W. L., M. A. Moran, W. M. Sheldon, R. G. Zepp and S. Opsahl, 2002. Determination of apparent quantum yield spectra for the formation of biologically labile photoproducts. Limnol. Oceanog. **47:** 343–352.

Moffett, J. W. and R. G. Zika, 1983. Oxidation kinetics of Cu(I) in seawater: implications for its existence in the marine environment. **13:** 239–251.

Moffett, J. W. and O. C. Zafiriou, 1993. The photochemical decomposition of hydrogen peroxide in surface waters of the eastern Caribbean and Orinoco River. Journal of Geophysical Research **98:** 2307–2313.

Mopper, K. and X. Zhou, 1990. Hydroxyl radical photoproduction in the sea and its potential impact on marine processes. **250:** 661–664.

Moran, M. A. and R. G. Zepp, 1997. Role of photoreactions in the formation of biologically labile compounds from dissolved organic matter. Limnology and Oceanography **42:** 1307–1316.

Moran, M. A., W. M. Sheldon and R. G. Zepp, 2000. Carbon loss and optical property changes during long-term photochemical and biological degradation of estuarine dissolved organic matter. Limnology and Oceanography **45:** 1254–1264.

Morehouse, K. M., W. D. Flitter and R. P. Mason, 1987. The enzymatic oxidation of Desferal to a nitroxide free radical. **222:** 246–250.

Morel, F. M. M. and J. G. Hering, 1993. Principles and Applications of Aquatic Chemistry, John Wiley & Sons, Inc., New York, pp. 421–508.

Pochon, A., P. P. Vaughan, D. Gan, P. Vath, N. V. Blough and D. E. Falvey, 2002. Photochemical oxidation of water by 2-methyl-1,4-benzoquinone: evidence against the formation of free hydroxyl radical. Journal of Physical Chemistry A **106:** 2889–2894.

Qian, J., K. Mopper and D. J. Kieber, 2001. Photochemical production of the hydroxyl radical in Antarctic waters. Deep-Sea Research I **48:** 741–759.

Schwarzenbach, R. P., P. M. Gschwend and D. M. Immboden, 1993. Environmental Organic Chemistry, John Wiley and Sons, Inc., New York, pp. 436–484

Scully, N. M., D. J. McQueen, D. R. S. Lean and W. J. Cooper, 1996. Hydrogen peroxide formation: the interaction of ultraviolet radiation and dissolved organic carbon in lake waters along a 43-75° gradient. **41:** 540–548.

Southworth, B. A. and B. M. Voelker, 2003. Hydroxyl Radical Production via the Photo-Fenton Reaction in the Presence of Fulvic Acid. Environmental Science and Technology **37:** 1130–1136.

Staehelin, J. and J. Hoigné, 1985. Decomposition of ozone in water in the presence of organic solutes acting as promoters and inhibitors of radical chain reactions. Environmental Science and Technology **19:** 1206–1213.

Stookey, L. L., 1970. Ferrozine – a new spectrophotometric reagent for iron. Analytical Chemistry **42:** 779–781.

Takahashi, N., T. Nakai, Y. Satoh and Y. Katoh, 1995. Ozonolysis of humic acid and its effect on decoloration and biodegradability. Ozone: Science & Engineering **17:** 511–525.

Valentine, R. L. and R. G. Zepp, 1993. Formation of carbon monoxide from the photodegradation of terrestrial dissolved organic carbon in natural waters. Environmental Science and Technology **27:** 409–412.

Vaughan, P. P. and N. V. Blough, 1998. Photochemical formation of hydroxyl radical by constituents of natural waters. Environmental Science and Technology **32:** 2947–2953.

Voelker, B. M. and D. L. Sedlak, 1995. Iron reduction by photoproduced superoxide in seawater. Marine Chemistry **50:** 93–102.

Voelker, B. M. and B. Sulzberger, 1996. Effects of fulvic acid on Fe(II) oxidation by hydrogen peroxide. Environmental Science and Technology **30:** 1106–1114.

Voelker, B. M., F. M. M. Morel and B. Sulzberger, 1997. Iron redox cycling in surface waters: effects of humic substances and light. Environmental Science and Technology **31:** 1004–1011.

Wang, G. S., C. H. Liao and F. J. Wu, 2001. Photodegradation of humic acids in the presence of hydrogen peroxide. Chemosphere **42:** 379–387.

Westerhoff, P., G. Aiken, G. Amy and J. Debroux, 1999. Relationships between the structure of natural organic matter and its reactivity towards molecular ozone and hydroxyl radicals. **33:** 2265–2276.

White, E. M., 2000. Determination of photochemical production of hydroxyl radical by dissolved organic matter and associated iron complexes in natural waters. M.S. Thesis, The Ohio State University, Columbus, OH.

Zafiriou, O. C. and M. B. True, 1979. Nitrate photolysis in seawater by sunlight. Marine Chemistry **8:** 33–42.

Zafiriou, O. C. and M. B. True, 1979. Nitrite photolysis in seawater by sunlight. Marine Chemistry **8:** 9–32.

Zafiriou, O. C. and R. Bonneau, 1987. Wavelength-dependent quantum yield of OH radical formation from photolysis of nitrite ion in water. Photochemistry and Photobiology **15:** 723–727.

Zellner, R., M. Exner and H. Herrmann, 1990. Absolute OH quantum yields in the laser photolysis of nitrate, nitrite and dissolved H_2O_2 at 308 and 351 nm in the temperature range 278–353 K. Journal of Atmospheric Chemistry **10:** 411–425.

Zepp, R. G., 1982. Experimental approaches to environmental photochemistry. In: O. Hutzinger (ed.) The Handbook of Environmental Chemistry, Springer-Verlag, Berlin, pp. 19–41.

Zepp, R. G., J. Hoigné and H. Bader, 1987. Nitrate-induced photoxidation of trace organic chemicals in water. Environmental Science and Technology **21:** 443–450.

Zepp, R. G., B. C. Faust and J. Hoigné, 1992. Hydroxyl radical formation in aqueous reactions (pH 3-8) of iron (II) with hydrogen peroxide: the photo-Fenton reaction. Environmental Science and Technology **26:** 313–319.

Zepp, R. G., M. M. Gumz, W. L. Miller and H. Gao, 1998. Photoreaction of valerophenone in aqueous solution. Journal of Physical Chemistry A **102:** 5716–5723.

Zepp, R. G., 2002. Solar ultraviolet radiation and aquatic carbon, nitrogen, sxulfur and metals cycles. In: E. W. Helbling and H. Zagarese (eds.), UV effects in aquatic organisms and ecosystems, Royal Society of Chemistry, Cambridge, UK, pp. 137–183.